Available online at www.sciencedirect.com
ScienceDirect
Applied Geochemistry 22 (2007) 30–52
Applied Geochemistry
www.elsevier.com/locate/apgeochem

The cycling of Ni, Zn, Cu in the system "mine tailings–ground water–plants": A case study

Nikolay V. Sidenko *, Elena I. Khozhina, Barbara L. Sherriff

Department of Geological Sciences, University of Manitoba, Winnipeg, Man., Canada R3T 2N2

Received 14 July 2005; accepted 28 July 2006
Editorial handling by B. Wang
Available online 20 November 2006

Abstract

The comparative behaviour of Ni, Cu and Zn in the system "mine tailings–ground water–plants" has been investigated at the Ni–Cu mine site operated by INCO Ltd. Thompson Operations, Thompson, Manitoba. Oxidation of sulphide minerals causes the release of metals from exposed tailings containing Ni ~2000 ppm, Cu ~150 ppm and Zn ~100 ppm to the ground water, which contains 350 mg/L Ni, 0.007 mg/L Cu, and 1.6 mg/L Zn. The metal concentration in the ground water is affected by the relative proportions of sulfide minerals, the rate of oxidation of sulphide minerals (Ni-bearing pyrrhotite > sphalerite > chalcopyrite), and the affinity of the metals for secondary Fe-phases (Ni > Zn > Cu).

Metals bound to Fe-phases are unavailable for plants, whereas water-soluble, exchangeable and carbonate bound metals in the tailings are considered to be available. The available Ni (340 ppm) was found to be significantly greater than available Cu (2.3 ppm) and Zn (2.5 ppm). The concentration of Ni (290 ppm), in the root system of water sedge (*Carex aquatilis* Wahl.) is about the same as in the available fraction, whereas Cu and Zn in the roots are higher (42 and 21 ppm, respectively). Therefore, Cu and Zn seem to be actively absorbed by the plants, while Ni diffuses passively into the roots. Nickel and Zn penetrate from the root into the shoot system more readily than Cu. After death, the shoots of the plants from the tailings still accumulate metals to give concentrations of Ni (850 ppm), Cu (97 ppm), and Zn (23 ppm) which were greater than those in the roots and living shoots. In an uncontaminated area, shoots do not absorb metals after death.

1. Introduction

The mining of base metals produces large quantities of fine-grained sulfide waste. If the waste is exposed to the atmosphere, sulfide oxidation can release metals and contaminate groundwater (Blowes and Ptaček, 1994; Johnson et al., 2000) or aquatic ecosystems (Marques et al., 2001). Exposed sulfide tailings often form barren landscapes with a few plants surviving in an environment lacking in nutrients and with a high load of potentially toxic metals (Winterhalder, 1995; Tisch et al., 1999; Newman et al., 2005). Vegetation growing on the mine waste can accumulate significant concentrations of metals, causing penetration into food webs (Cobb et al., 2000; Khozhina, 2002). Accumulation of a specific metal in a plant depends on the availability

* Corresponding author.
E-mail address: sidenkon@cc.umanitoba.ca (N.V. Sidenko).

0883-2927/$ - see front matter © 2006 Elsevier Ltd. All rights reserved.
doi:10.1016/j.apgeochem.2006.07.019

of the metal and the physiological barriers within the plant (Salisbury and Ross, 1992; Brooks, 1983). The concentration of available metals depends on the metal speciation in solids (Fergusson, 1990; Raven et al., 1999; Kabata-Pendias and Pendias, 2001). In this study, the authors compare the transport of Ni, Cu and Zn through the system "mine tailings–ground water–plants". The approach was to determine metal speciation in the tailings and analyse different parts of the plants collected from the Ni–Cu mine site at INCO Ltd. Thompson, Manitoba.

The mine is located about 5 km south of the town of Thompson (55°38′N, 97°9′W, Fig. 1(a)). This region has a continental climate typical of Central Canada with a short frost-free season (about 85 days). It is in the Boreal Forest region and the vegetation consists mostly of stunted trees and low bush (Klohn Leonoff, 1992).

INCO ltd. mines three deformed stratabound ore bodies contained within metasediments (SRK, 1984). The ore consists of pentlandite, chalcopyrite, and Ni-pyrrhotite with minor pyrite, violarite and mackinawite. The processing of the ore includes milling, selective flotation, and smelting of flotation concentrates. Since 1960, about 40 million tonnes of flotation tailings have been produced by INCO Ltd. and have been discharged into the Tailings Management Facility. Most tailings are kept submerged, but about 3 km^2 of topographically high areas have been left exposed (Fig. 1(b)). The tailings contain from 4.0 to 15.7 wt.% S (Klohn Leonoff, 1992). Sulfide minerals are predominantly Ni-bearing pyrrhotite, with minor pyrite, chalcopyrite, sphalerite and pentlandite in an assemblage with the gangue minerals biotite, quartz, and feldspar with minor amphibole and calcite. The net neutralizing potential (NNP) of the tailings varies from −91.5 to −458 kg $CaCO_3$ eq/t (Klohn Leonoff, 1992).

2. Methods

2.1. Sampling

In order to study lateral and vertical zoning, a trench was dug by bulldozers through tailings deposited 5–10 a ago (Fig. 1(c)). Trench walls were smoothed at 14 observation points where the stratification was documented using a Munsell® chart to describe color. At four points (Figs. 1(c) and 2), representative samples were collected from vertical sections, and then sealed in polyethylene bags. The sample number includes the section number and sample number, starting from the deepest upwards (e.g., 1/6 is the top sample #6 from section 1, Fig. 2). The deepest sample from each section was collected with an auger from the saturated zone, where oxidation of sulfides should be minimal. Therefore, there are gaps between auger samples and the continuous upper part of the sections

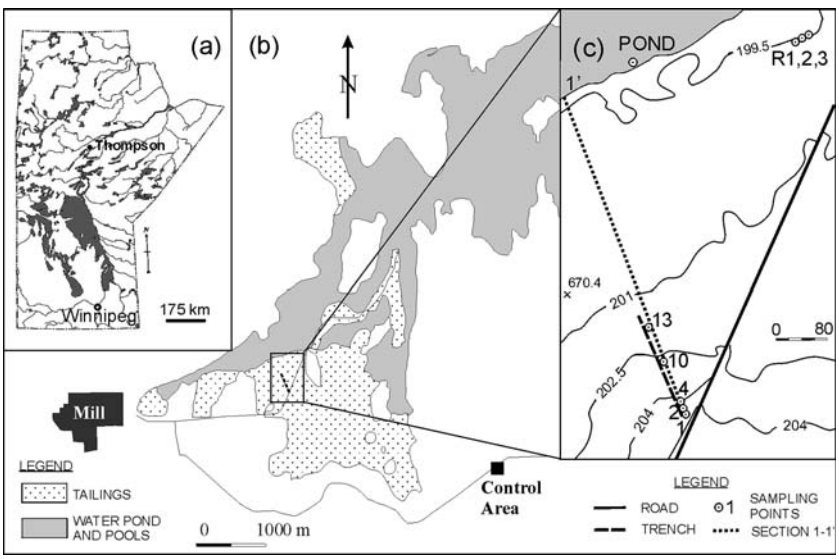

Fig. 1. (a) A map showing the location of the INCO Ltd. Ni–Cu mine in Thompson, Manitoba. (b) A plan of the tailings showing the trench and (c) the sampling points.

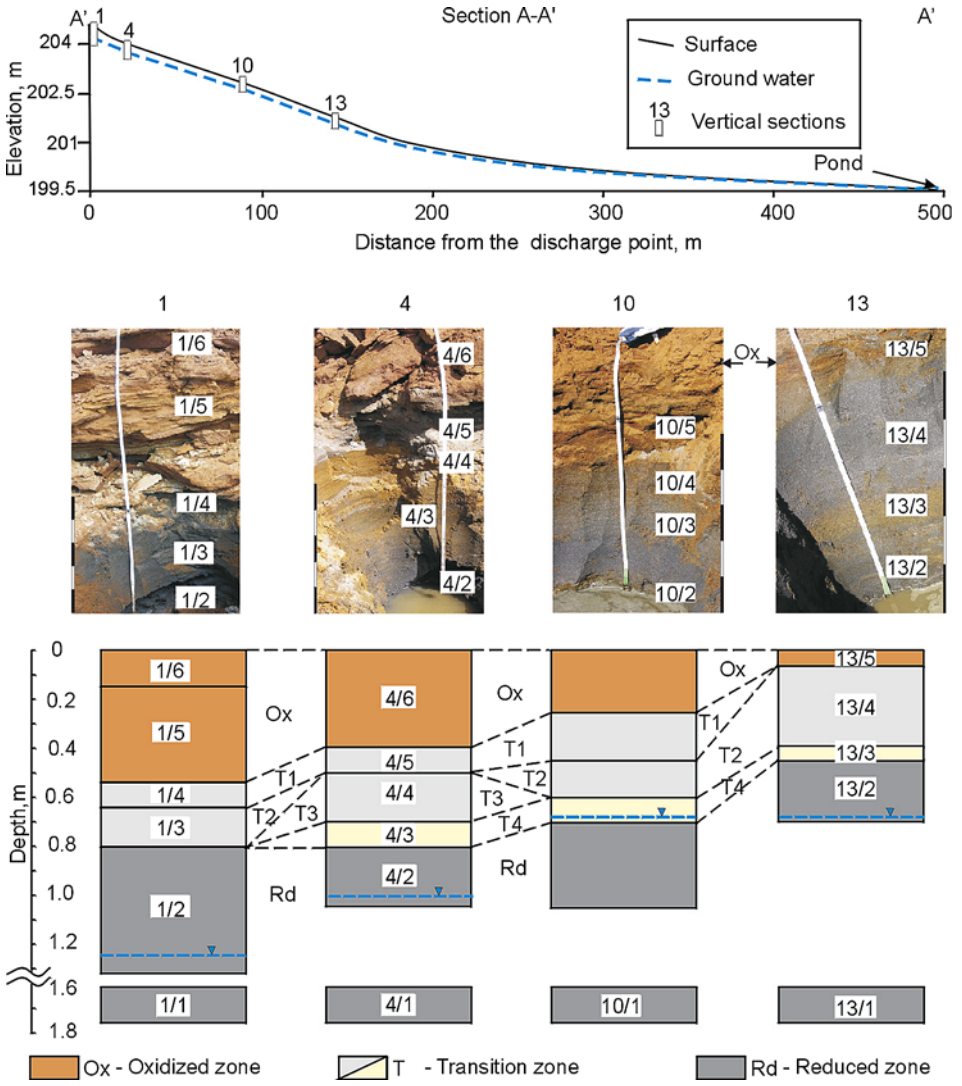

Fig. 2. The position of the vertical sections and the location of samples in these sections. The correlation of zones between different sections of the trench. Zone names: Ox – Oxidized zone, T1–T4 – Transition zone, Rd – Reduced zone. The dashed line with triangles shows the level of the water table.

(Fig. 2). Samples of evaporite minerals and weathered mica were collected from the surface, and placed in sealed vials to prevent possible dehydration and oxidation.

Ground water was sampled from the bottom of pits 1, 4 and 13 dug in the trench to the saturated zone. Only the shallow groundwater at the interface of the saturated and exposed tailings has been studied. Neither deep ground water within the tailings nor ground water from the silt and clay below or outside of the tailings body were collected. Water was also collected from the tailings pond to compare with groundwater (Fig. 1(c)). The water was passed through a 0.45 μm filter before being divided into three aliquots; the first was acidified with concentrated HNO_3 (2 mL/L) to preserve metals in solution, the second with 6 M HCl (1 mL/60 mL) for determination of Fe species and the third stored unacidified for anion determination. All samples were stored at 10 °C until analyzed by Envirotest Laboratories Ltd.

Samples of natural soil were collected from four points (<20 cm depth) within an uncontaminated control area, 3.5 km south of the trench (Fig. 1(b)). The clay soils in this region are of glacial–lacustrine origin. They were produced by

weathering of metamorphic rocks, which had contained some traces of sulfide minerals.

Water sedge plants (*Carex aquatilis* Wahl.) were collected from the control area and from the tailings (Fig. 1(c)). One population of the plants, which was growing in the tailings, had developed as a series of rings with oldest plants (R3) in the centre, surrounded by the next oldest (R2) and the youngest (R1) forming new growths further out into the tailings (Fig. 3). From 15 to 20 plants were collected from each of these three circles (R1, R2 and R3) by digging. Roots were collected from a soil volume of about $30 \times 30 \times 30\ cm^3$, which allowed sampling of the majority of the biomass of roots. The plants were washed first in pond water and then in distilled water before being divided into separate parts; root system, live and dead shoots. Plants were sampled in the beginning of July when live shoots consisted mainly of leaves. Leaves, which had died in the previous season, but were still standing and attached to the roots, were separated from the roots to be compared to the leaves that were still alive. At the end of September, seeds of water sedge were collected for germination tests from both the tailings and control area.

2.2. Analyses

Solid samples were air dried and portions were sent to Vancouver Petrographics Ltd. to be made into polished thin sections, using oil for cutting and grinding to minimize the dissolution of water-soluble minerals. A second portion was crushed and passed through a <65 μm sieve to obtain the fine fraction as this would be enriched in secondary minerals with respect to the coarser fraction. A third portion was ground to <5 μm for sequential extraction.

Minerals were identified in <65 μm fraction of tailings, and in samples of evaporites and weathered mica using a Phillips PW 1729 powder X-ray diffractometer (XRD) operated under Ni-filtered Cu-Kα radiation. Scans were recorded from 3° to 70°, 2θ with steps of 0.05°, at a rate of 1.5° 2θ per min.

Polished sections were studied using optical microscopy in reflected and transmitted light. Mineral grains were also observed with a scanning electron microscope (SEM, Stereoscan 120, Cambridge Instruments), and analyzed qualitatively with an X-ray energy-dispersive spectral analyzer (EDS). Quantitative analysis of minerals was done with a Cameca SX 100 electron microprobe (EMP)

Fig. 3. Water sedge plants in tailings area showing the sampling points R1–3.

operated with a 2 μm diameter beam at an acceleration potential of 15 kV and a beam current of 20 nA. The set of elements chosen for EMP analysis was based on the SEM-EDS data, and used chalcopyrite (S), magnetite (Fe) and elemental Ni standards. Detection limits for different elements varied from 0.01 to 0.05 wt.%, with analytical precision being ≈2%.

A sequential extraction procedure was used to determine the speciation of Fe, S, Ni, Cu, and Zn in samples of the tailings. The technique was initially developed for lake sediments (Tessier et al., 1979) and later applied to mine tailings (McGregor et al., 1995; Ribet et al., 1995; Fanfani et al., 1997; Dold and Fontboté, 2001). One gram of <5 μm powder was placed into a 50 mL centrifuge tube and dissolved sequentially in different reagents as described below. After each step of the extraction (a)–(d), the solid residue was separated from the liquid by centrifuging at 2000 rpm for 20 min, and the solution passed through a 0.2 μm filter. The residue was rinsed with 5 mL of distilled water, which were centrifuged and added to the solution.

(a) The water-soluble fraction was extracted by agitation with 40 mL distilled water for 1 h at room temperature. This step liberates elements from the most soluble phases of tailings such as hydrated sulfates of Ni, Cu and Zn (Dold, 2003a; Sidenko et al., 2005).
(b) Carbonates and exchangeable metals were leached with 30 mL of 1 M NH_4–acetate solution, buffered at pH 4.5 by acetic acid, for 3 h at room temperature (Hall et al., 1996; Dold, 2003a). This leach mobilizes metals from carbonates, exchangeable cations from phyllosilicates and elements weakly absorbed onto the surface of Fe-oxyhydroxides. This fraction represents the portion of metals, which can be available for plants (Tan, 1996).
(c) Metals bound to amorphous and poorly crystalline Fe-phases were extracted by 30 mL of 0.2 M NH_4–oxalate solution, adjusted with oxalic acid at pH 3.2 in the dark, after Chao and Zhou (1983). The leaching process continued for 1, as this period was considered to be sufficient for complete dissolution of schwertmannite ($Fe_8O_8(OH)_{8-2x}(SO_4)_x \cdot nH_2O$) and ferrihydrite ($5Fe_2O_3 \cdot 9H_2O$) (Dold, 2003b).
(d) Elements co-precipitated with well crystalline phases of Fe such as goethite (FeOOH) and jarosite ($KFe_3(SO_4)_2(OH)_6$) were extracted by 45 mL of 1 M $NH_2OH \cdot HCl$ solution in 25 vol.% acetic acid at <96 °C (Hall et al., 1996). It was determined, from a XRD study of the solid residue, that 6 h were sufficient to dissolve these phases.
(e) The residual fraction was calculated to be the difference between the total content and the sum of concentrations from steps (a)–(d). This fraction contains elements bound to primary minerals, which are mainly sulfides.

To determine the total content of Fe, S, Ni, Cu and Zn in the tailings and natural soils, 0.5 g of the air-dried samples were dissolved using the HF/HNO_3/$HClO_4$ digestion technique (Bock, 1984). For natural soils, the water-soluble, and exchangeable/carbonate fractions of metals were extracted with steps (a) and (b) of the leaching technique. Blanks were used to account for possible contributions from the reagents.

The concentrations of the elements in all leachates were measured, using a Varian Liberty 200, inductively coupled plasma, optical emission spectrometer (ICP-OES) referenced to ICP standard solutions (SCP Science®) at the Department of Geological Sciences, University of Manitoba. The precision of the sequential extraction technique was tested by triplicate analyses of sample # 13/4 of the tailings (Table 1).

For water samples, Eh and pH were measured immediately after collection using an AP-62 pH/Eh meter with an OPR-97-87 (Thermo ORION) Pt electrode for Eh with an accuracy of ±5 mV and a 13-620-AP50 (Accumet) Ag/AgCl pH electrode with an accuracy of ±0.02 pH units. The pH of natural soils and tailings were measured on 10 mL of an air dried, <2 mm grain-size sample mixed with 20 mL distilled water (1:2 soil–water ratio, Lierop, 1990). The mixture was allowed to stand for 30 min before the pH was measured.

Water samples were analyzed for total metal concentrations by inductively coupled plasma mass spectroscopy (ICP-MS), and for SO_4^{2-} by turbidimetry. Ion chromatography (IC) was used to measure Cl and F concentrations. The precisions of these techniques is within 10%. Bicarbonate alkalinity was not measured for groundwater because the pH was <4.5. Divalent and trivalent Fe species were separated using ion chromatography, followed by

Table 1
Analyses in triplicate of speciation of elements in tailings sample # 13/4

Sample	Total ppm	Water-soluble		Exch. + carbon.		Am. Fe-hydrox.		Cry. Fe-hydrox.	
		ppm	% of tot.	ppm	% of tot.	ppm	% of tot.	ppm	% of tot.
Fe									
13/41	80 300	1290	1.6	270	0.3	13 200	16	21 100	26
13/42	93 100	1300	1.4	130	0.1	15 900	17	21 200	23
13/43	110 700	1290	1.2	240	0.2	15 100	14	20 700	19
Mean	94 700	1293	1.4	213	0.2	14 733	16	21 000	23
SD	15 300	5.8	0.2	74	0.1	1387	2	300	3.8
S									
13/41	59 600	4920	8	250	0.42	230	0.4	690	1.2
13/42	44 200	4860	11	220	0.50	310	0.7	680	1.5
13/43	45 400	4930	11	220	0.48	250	0.6	650	1.4
Mean	49 733	4903	10	230	0.47	263	0.5	673	1.4
SD	8600	38	2	17	0.04	42	0.2	21	0.2
Ni									
13/41	1200	250	21	20	1.6	73	6.1	132	11.0
13/42	1100	250	23	21	1.9	88	8.0	131	11.9
13/43	1500	260	17	21	1.4	88	5.8	130	8.6
Mean	1267	253	20	20	1.6	83	6.6	131	10.5
SD	210	6	3	0.7	0.3	9	1.2	1.0	1.7
Cu									
13/41	118	<0.1	<0.1	2.1	1.8	3.0	2.5	35.1	30
13/42	106	<0.1	<0.1	1.4	1.3	3.1	3.0	35.0	33
13/43	117	<0.1	<0.1	2.0	1.7	3.3	2.8	34.1	29
Mean	114	<0.1	<0.1	1.8	1.6	3.1	2.8	34.7	31
SD	7	–	–	0.4	0.3	0.2	0.2	0.6	2
Zn									
13/41	71	1.9	2.7	0.6	0.8	9.3	13	18.2	26
13/42	67	1.9	2.8	0.6	0.9	11.2	17	18.4	28
13/43	75	2.0	2.7	0.5	0.7	11.0	15	18.2	24
Mean	71	1.9	2.7	0.6	0.8	10.5	15	18.3	26
SD	4	0.1	0.1	0.1	0.1	1.1	1.8	0.1	1.7

spectrometric analysis of total Fe. The precision of this analysis is 10–15% depending on the Fe concentration and the matrix of the solution.

The distribution of the saturation indices of minerals in the ground and surface water were calculated using the WATEQ4f computer program (Ball and Nordstrom, 1991). The analytically determined Fe^{2+}/Fe^{3+} ratios were used to calculate the activities of Fe and Cu redox couples.

Samples of shoots and roots were air-dried and macerated in a coffee-grinder. Portions of the crushed plant material, 2.5 g in weight, were digested with HF/HNO_3 (Bock, 1984) and analysed for Ni, Cu and Zn using ICP-OES. The precision of the analyses is 10% of the total concentration. Mean value of the metal concentration [Me] of the plant body was calculated from the metal concentration $[Me]_i$ and the dry weight (m_i) of each part (i), and the dry mass of the plant [M]:

$$\frac{1}{M} \cdot \sum_i [Me]_i \cdot m_i = [Me].$$

Seed germination was tested according to the techniques of Bradbeer (1988), and Koval and Shamanin (1999). Seeds were stratified to induce germination by placing 100 seeds in a 90 mm diameter sterile Petri dish on wet filter paper. The Petri dishes were placed in a growth chamber at 25 °C for 24 h and than in a cold room at 2 °C for another 24 h (Koval and Shamanin, 1999). This cycle was repeated once more. Stratified seeds were germinated in a growth chamber for two weeks at 23 °C during light period of 16 h, and at 18 °C during dark period of 8 h. During the stratification and

germination of seeds the filter paper in Petri dishes was kept wet. Three replicate tests were made for seeds from each of the tailings and control areas.

3. Results

3.1. Lithology and mineralogy

The following zones are based on the observations of physical properties and the degree of mineral alteration from 14 cross-sections. Three principal zones were identified; reduced, transition and oxidized. The transition zone contains several layers distinguished by macroscopic features (Fig. 2). These layers are labelled T1–T4.

The reduced zone is usually below the water table (Fig. 2). In this zone, the tailings are loose and saturated with water (Fig. 2) and vary in colour from dark bluish grey (GLEY2 4/1) to bluish black (GLEY2 2.5/1). They consist mainly of primary minerals, reflecting the original composition of the sulfide waste (Table 2). However, some pyrrhotite grains have been replaced by marcasite (Fig. 4(a)) and thin films of Fe hydroxides surround some sulfide grains. Products of sulfide oxidation, such as jarosite and S, were identified in samples collected

Table 2
Characteristics of layers in trench section # 4

Sample #	Zone	Depth (cm)	Colour	Munsell index	Major minerals[a]
TR-4/6	Ox	0–40	Yellowish brown	10YR 5/4	Quartz, sulphur, goethite, lepidocrocite
TR-4/5	T1	40–50	Light bluish grey	GLEY2 8/1	Quartz, goethite, jarosite, sulphur
TR-4/4	T3	50–70	Yellow	10YR 7/8	Sulphur, quartz, jarosite, goethite
TR-4/3	T4	70–80	Olive yellow	2.5Y 6/6	Pyrrhotite, quartz, sulphur, goethite, lepidocrocite
TR-4/2	Rd	80–100	Dark bluish grey	GLEY2 4/1	Pyrrhotite, biotite, sulphur, jarosite
TR-4/1	Rd	160–175	Bluish black	GLEY2 2.5/1	Quartz, pyrrhotite, biotite,

[a] Identified by XRD in >65 μm fraction of the samples.

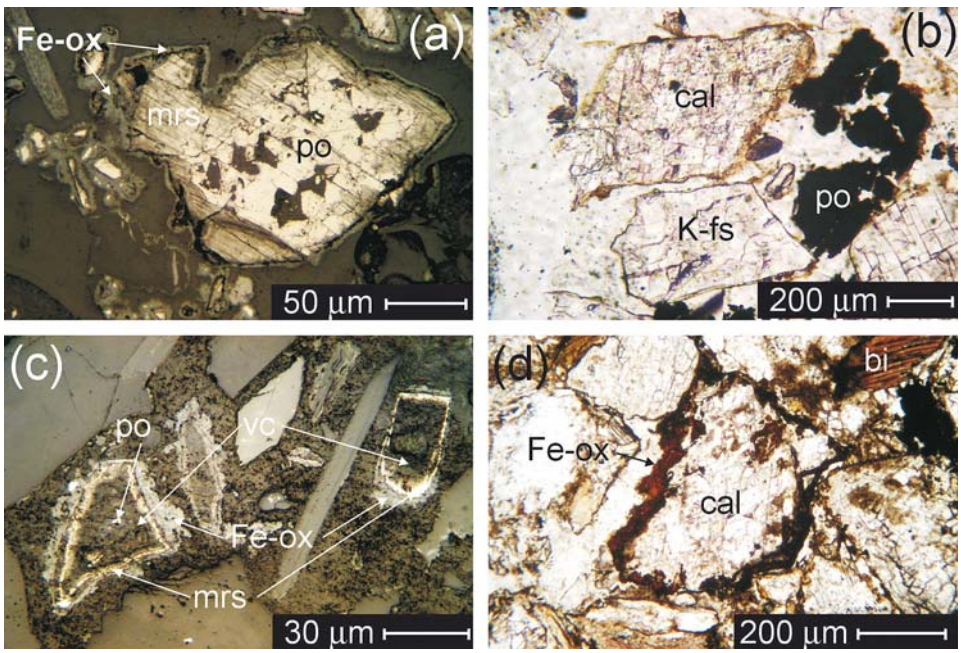

Fig. 4. Photomicrographs of polished thin sections in (a), (c) reflected and (b), (d) transmitted plane polarized light, showing: (a) pyrrhotite (po) partially replaced by marcasite (mrs) and Fe-oxyhydroxides (Fe-ox) in sample 4/2; (b) an unaltered calcite (cal) grain in contact with pyrrhotite and K-feldspar (K-fs) from sample 4/2; (c) the atoll-like texture of pyrrhotite grains almost surrounded by vacant zone (vc), marcasite and Fe-oxyhydroxides in sample 4/3 and (d) a corroded calcite grain is surrounded by Fe-oxyhydroxides in sample 4/3.

at the level of the water table. Calcite grains are angular and do not show dissolution features, but occasionally they are coated by a thin red film of Fe hydroxide (Fig. 4(b)).

The transition zone extends to a maximum of 1 m above the water table (Fig. 2). Material of this zone is loose and less saturated with water than the reduced zone. There are often different colored layers. Olive-yellow (2.5Y 6/6) T4 or brownish-yellow (10YR 6/6) T3 beds are usually observed at/or just above the water table, marking the precipitation of goethite, lepidocrocite and S (Table 2). Bluish grey (GLEY2 6/1) T2 layers and light bluish grey (GLEY2 8/1) or pale brown (10YR 8/3) T1 layers are found as the top sequence in most sections.

In the transition zone, about 50% of pyrrhotite is replaced by secondary minerals. The rims become more complex then in the reduced zone. The sequence "pyrrhotite–vacant zone (epoxy filled)–marcasite–Fe oxide" found from the core to the outer rim of oxidized pyrrhotite (Fig. 4(c)) is similar to zoning observed by Jambor (2003). There is evidence of pentlandite and sphalerite alteration, while pyrite and chalcopyrite grains do not show any evidence of oxidation. Calcite grains are corroded and surrounded by thick rims of Fe hydroxides (Fig. 4(d)).

The oxidized zone consists of reddish (5YR 5/4) to yellowish-brown (10YR 5/6), usually cemented, hardpan layers from a few cm to 0.5 m thick. This zone consists of reddish (5YR 5/4) to yellowish-brown (10YR 5/6), usually cemented, hardpan layers from a few cm to 0.5 m thick. The total thickness of the oxidized zone has an inverse relationship to the depth to the water table. The water table is apparently controlling the moisture content in the pore space, and hence the diffusion of O_2 and rate of sulfide oxidation.

The few marcasite rims observed around pyrrhotite grains in the oxidized zone are thin. Iron hydroxide rims, however, are thicker than in the transition zone and consist of inner rims replacing pyrrhotite and outer ones representing the cement (Fig. 5(a)). An EMP profile shows a decrease in the concentration of Ni from 0.56 wt.% in the core of a pyrrhotite grain through an inner rim of Fe hydroxide to 0.16 wt.% in the cement (Fig. 5(b)). Most of the pyrrhotite grains are replaced by secondary Fe phases, and pyrite is altered along fractures (Fig. 5(c)). Pentlandite and chalcopyrite show a minor replacement by Fe-oxyhydroxides. Goethite and lepidocrocite, identified by XRD in

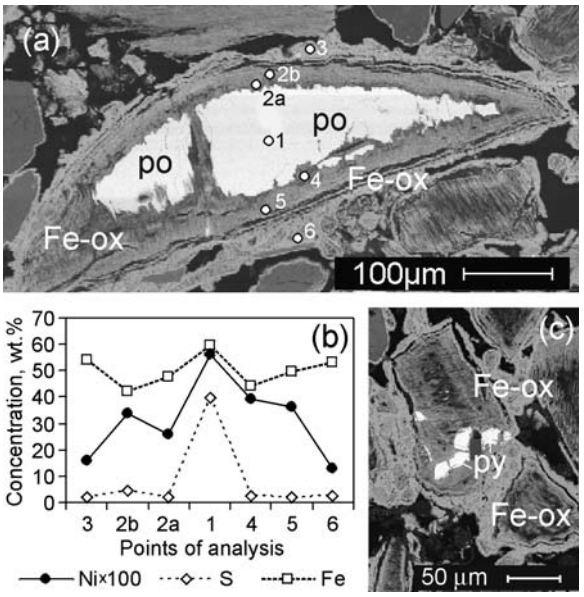

Fig. 5. SEM electron backscattered images and the results of EMP analyses showing: (a) pyrrhotite grain surrounded by Fe-oxyhydroxides with analytical points through a rim–core–rim profile from sample 1/4; (b) the concentration of Ni, S and Fe across the profile; (c) a grain of pyrrhotite almost completely replaced by Fe-oxyhydroxides containing inclusions of pyrite, sample 1/5.

the >75 μm fraction, are probably from the cement of the hardpan. Jarosite was mainly found in the lower part of the hardpan, while goethite and lepidocrocite were distributed irregularly (Kavalench, 2004). There was no calcite found in this zone using mineralogical methods.

The formation of green, white and yellow coloured crusts of evaporate minerals were observed on the surface of tailings during dry weather. Morenosite (Ni, Fe, Mg)$SO_4 \cdot 7H_2O$ and melanterite (Fe, Ni, Mg)$SO_4 \cdot 7H_2O$ were identified by powder XRD and SEM-EDS analyses. Weathered mica from the surface of tailings consists of interstratified biotite–vermiculite. These layers are estimated to be in the ratio 40:60 from the *d*-spacing of 13.4 Å for the combination of the 001/002 (biotitic/vermiculate) basal reflection (Moore and Reynolds, 1997).

3.2. Element speciation in the tailings

The weighted mean concentration of total Fe varies from 12 to 18 wt.% with the vertical distribution varying between sections (Fig. 6, Appendix 1). The mean proportions of Fe in the residual fractions show that from 63% to 66% of Fe remains in

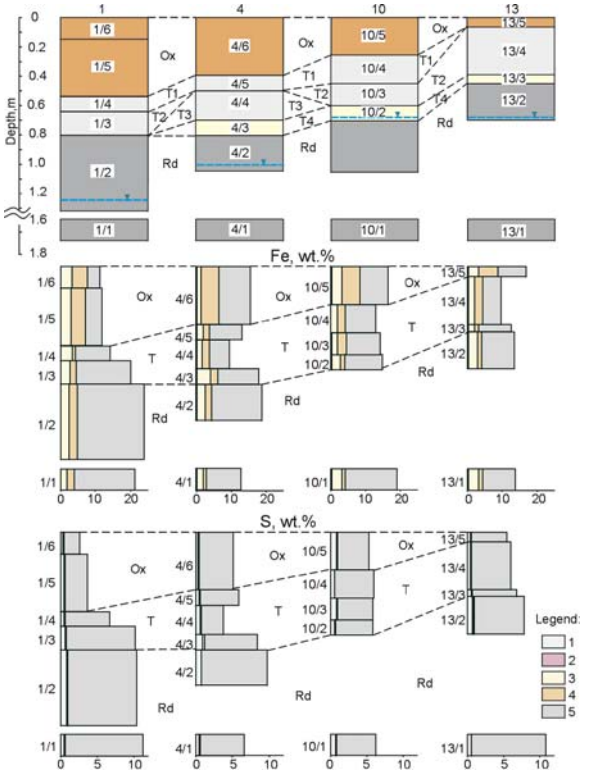

Fig. 6. Speciation of Fe and S in the tailing solids from sequential extraction. The fractions are (1) water-soluble fraction (2) exchangeable and carbonate, (3) bound to amorphous and poorly crystalline Fe-oxyhydroxides and oxyhydroxysulfates, (4) bound to crystalline Fe-oxyhydroxides and oxyhydroxysulfates and (5) residual.

sulfides, mainly in pyrrhotite. The dominant secondary forms are crystalline and amorphous Fe-oxyhydroxides (Appendix 1). Mean proportions of Fe in the crystalline form are slightly greater (18–20% of total Fe) then in the amorphous fraction (13–17% of total Fe). In all sections, the highest concentrations of crystalline Fe-oxyhydroxides are in the uppermost oxidized zone. Concentrations of amorphous Fe do not display a clear distribution pattern. The maximum of Fe concentrations of this fraction are found in the oxidized zone in sections 1 and 10, while in sections 4 and 13 they are in the T4 layer of the transition zone (Appendix 1).

The mean total S content varies from 5.5 wt.% to 7.5 wt.% between sections, with 87–90% of the total concentration in residual sulfides (Fig. 6) and 7–11% of the total concentration in the water-soluble fraction. The mean concentrations of S bound to secondary amorphous and crystalline Fe-oxyhydroxides are low and range from 0.04 to 0.06 wt.% and 0.06 to 0.08 wt.%, respectively. The distribution of this S species shows a clear pattern. The highest concentrations of S precipitated with amorphous Fe-oxyhydroxides are in the transition zone mainly in the T4 layer (sections 4, 10, 13), while maximum concentrations of S in secondary crystalline Fe minerals accumulate in the uppermost oxidized zone (Appendix 2).

Between sections, the weighted mean concentration of Ni ranges from 1600 to 2900 ppm with 60–73% being in the residual fraction (Appendix 3), reflecting the proportion of Ni still in primary minerals. The 3 major secondary forms accumulating Ni are soluble, amorphous and crystalline Fe phases, with means of 8–18%, 8–11% and 8–13%, respectively, of total concentrations. The highest values of water-soluble Ni (up to 23 of the total content) are in the transition zone (Fig. 7). The highest concentrations of Ni bound to amorphous Fe-phases, as well as in exchangeable and carbonate fractions is in the transition zone, particularly in the T4 layers (Fig. 7 and Appendix 3). The relation-

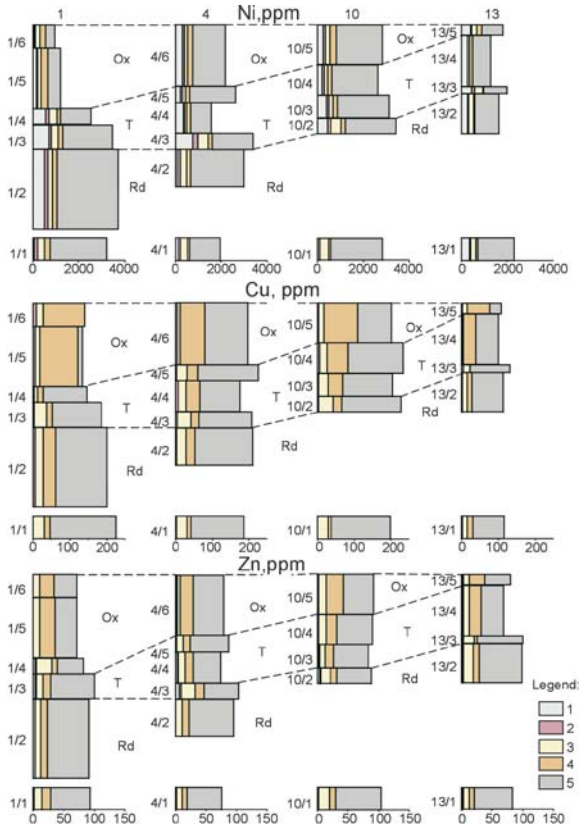

Fig. 7. The distribution of Ni, Cu and Zn in vertical sections of the tailings. The names of the fractions are the same as for Fig. 5.

ship between Ni in these fractions could be due to weakly adsorbed Ni being desorbed from the surface of amorphous Fe-phases during the extraction of exchangeable and carbonate fractions. Maxima of Ni concentrations bound to crystalline Fe-oxyhydroxides are in the oxidized zones of all sections (Appendix 3).

The mean Cu content is lower than Ni by one order of magnitude (120–220 ppm) with 52 to 69 water-soluble Cu in all samples of the tailings is below the detection limit (<0.1 ppm). Mean proportions of Cu in the exchangeable and carbonate fractions are low, 1.9–2.8% of total content. High concentrations of Cu in Fe-oxyhydroxides indicate the dominant secondary sink for the metal (Fig. 7). On average, Cu is predominantly concentrated in crystalline Fe-oxyhydroxides (mean 18–34%) compared to the amorphous phase (Appendix 4). The concentrations and proportions of Cu bound to crystalline Fe-oxyhydroxides increases upwards from the bottom of the transition zone in all sections being highest in the uppermost oxidized layer (Appendix 4). Maximum of Cu concentrations precipitated with amorphous Fe-phases were at the bottom of transition zone in close proximity to the water table (Appendix 4).

The mean concentrations of total Zn (81–92 ppm) are about half that of Cu. The proportion of Zn in the residual fraction indicates that from 60% to 67% of the total remains in primary minerals, mainly sulfides. The concentrations of Zn in soluble, exchangeable and carbonate fractions are low and insignificant (Appendix 5). From 29% to 36% of the total Zn is bound to secondary Fe-oxyhydroxides (Fig. 7) with the domination of crystalline (17–21% of total) over the amorphous fraction (12–15%). The concentrations of Zn bound to well ordered Fe-oxyhydroxides are highest in the oxidized zone of the tailings. High concentrations of Zn associated with amorphous Fe-phases are mainly accumulated in the lower part of sections, in the transition and reduced zones (Fig. 7).

3.3. Water chemistry

Shallow ground water travels radially from the cone of the tailings deposited at the discharge point towards the tailings pond (Fig. 2). The pH of ground water decreases systematically from 5.36 to 4.92 from TR13 to the more oxidized (TR2) area of the tailings (Table 3). The dominant anion in the ground water is SO_4^{2-} (Table 3) with the major cations being Fe^{2+} (1140–3250 mg/L), Mg^{2+} (1830–3160 mg/L), and Ca^{2+} (390–400 mg/L). A gradual increase in Ni concentrations from 3.6 to 607 mg/L and Cu from 0.005 to 0.009 mg/L were observed from TR13 to TR2. Zinc concentrations rise from 0.073 in TR13 to 2.55 mg/L in TR4. The tailings pond water is maintained at a neutral pH (7.65) and is characterized by a lower content of all components except Na, Cl^- and HCO_3^- (Table 3). Concentrations of Fe (0.15 mg/L), Ni (0.42 mg/L), Cu (0.003 mg/L) and Zn (<0.0005 mg/L) in the tailings pond water are significantly lower than in the ground water. This shows that the tailings are the major source of metals in the groundwater but not the tailings pond, which is still receiving effluent discharge from the mill and the smelter. The metal concentration in the pond is controlled by lime treatment of the effluent. Groundwater flowing from the more oxidized area mixes with the pond water, where it will be diluted and neutralized.

Table 3
Analyses of groundwater from trench pits and tailings pond (mg/L)

Sample	TR2	TR4	TR13	Pond
T (°C)	17.9	15.3	16.7	17.2
pH	4.92	5.29	5.36	7.65
Eh (V)	0.34	0.25	0.25	0.21
Ca	390	400	400	100
Mg	1830	1990	3160	26
Na	51.8	38.1	525	547
K	84.8	111	253	15
Cl^-	<0.05	23	137	342
F^-	<0.05	<0.05	<0.05	0.2
SO_4^{2-}	11 700	13 300	17 800	942
HCO_3^-	–	–	–	55
Fe total	1410	2950	3540	0.15
Fe^{2+}	1140	2220	3250	<0.1
Fe^{3+}	95.1	223	187	<0.1
B	0.28	0.30	0.92	3.18
Al	3.41	0.10	0.34	0.04
As	0.009	0.037	0.02	0.002
Ba	0.035	0.041	0.026	0.019
Cd	0.005	0.0007	0.0002	<0.0001
Co	4.25	2.83	0.013	0.004
Cu	0.009	0.007	0.005	0.003
Li	0.50	0.52	0.44	0.009
Mn	21.2	23.8	18.8	0.0744
Ni	607	441	3.6	0.42
Pb	0.0009	0.0001	0.0031	0.0005
Rb	0.46	0.44	0.22	0.019
Se	0.008	0.008	0.01	0.003
Sr	0.71	0.67	1.74	0.81
U	0.016	0.008	0.0013	0.0003
Zn	2.31	2.55	0.073	<0.0005

Calculated saturation indices (SI) indicate that the ground waters are supersaturated with respect to jarosite (SI = 12.7–14.3), goethite (SI = 8.6–8.9), and ferrihydrite (SI = 3.0–3.8). The saturation indices of soluble sulfates of Fe and Mg such as melanterite (SI = −1.9 to −1.4) and epsomite ($MgSO_4 \cdot 6H_2O$, SI = −1.5 to −1.2) are negative but close to zero, indicating that these minerals could precipitate if the solution evaporated.

3.4. Natural soils

The mean concentrations of Ni and Cu in the natural soils are 12 and 4 times lower than in the tailings although concentrations of Zn are similar (Table 4 and Appendices 3–5). The concentration of available Cu and Zn in natural soils (the sum of water-soluble, exchangeable and carbonate fractions) is similar to the tailings (Table 4, Appendices 4 and 5) whereas available Ni is 24 times lower. For natural soils the mean pH of 1:2 soil–water mixtures was 6.3 in comparison to 4.0 for the oxidised zone of the tailings and 7.2 for the reduced zone.

3.5. Plants

There is a much wider variety of species in the control area compared to the tailings. As water sedge (*Carex aquatilis* Wahl.) dominates within the exposed tailings, it was chosen for analysis. In the tailings, water sedge plants grow preferentially in the vicinity (~10 m) of natural woodlands and spread radially by roots, which grow longer than 75 cm to reach the groundwater. At the end of September, water sedge plants in the control area were dispersing ripe seeds in contrast to the plants from the tailings, where some seeds were still green. Seeds of water sedge collected from the exposed tailings have a low viability (14.0 ± 2.1% germination) compared to those from the control area (54.0 ± 8.9% germination).

The calculated mean concentration of Ni (260 ppm) in the plant body (live parts) from the tailings area is an order of magnitude greater than for Cu and Zn (Table 5). In contrast, in the con-

Table 4
Metal content in natural soils (ppm)

Sample #	Ni	Cu	Zn
Total			
CA1	90	38	75
CA2	100	42	85
CA3	49	23	74
CA4	270	62	47
Mean	130	41	70
Available[a]			
A1	20	5.6	7.35
CA2	7.1	<0.35	4.9
CA3	26	4.55	3.85
CA4	1.5	<0.35	<0.35
Mean	14	2.7	4.1

[a] Available form is ∑ water-soluble, exchangeable and carbonate fractions.

Table 5
Metal concentration in water sedge (ppm dry wt.)

	Ni	Cu	Zn
Tailings area			
Root system			
Ring 3	340	54	17
Ring 2	280	26	24
Ring 1	240	46	23
Mean	290	42	21
Live shoots			
Ring 3	150	7.9	15
Ring 2	120	7.3	17
Ring 1	330	11	17
Mean	200	8.7	16
Dead shoots			
Ring 3	1200	110	24
Ring 2	510	83	21
Ring 1		Was not found	
Mean	850	97	23
Entire plant (live organs)			
Ring 3	288	41	16
Ring 2	203	17	21
Ring 1	288	27	20
Mean	260	28	19
Control area			
Root system			
CA1	13	43	23
CA2	14	110	40
Mean	13	76	31
Live shoots			
CA1	8.0	14	14
CA2	10	23	18
Mean	9.0	18	16
Dead shoots			
CA1	4.9	19	11
Entire plant (live organs)			
CA1	11	29	19
CA2	13	77	32
Mean	12	53	25

trol area, Ni (12 ppm) is less than half the Cu and Zn concentrations. Ni concentration in plants from the tailings is 20 times greater than for the control area (Table 5). The mean concentrations of Ni (290 ppm), Cu (42 ppm) and Zn (21 ppm) in the root system are greater than in the live shoots (Ni – 200, Cu – 8.7 and Zn – 16 ppm). The difference between Cu concentrations in the root and shoot systems suggests the presence of a barrier for Cu between them. The concentrations of Ni (850 ppm), Cu (97 ppm), and Zn (23 ppm) are higher in dead shoots than in live shoots and roots.

In the control area, the concentrations of metals in the root system, live and dead shoots decrease in the order Cu > Zn > Ni (Table 5). The higher concentrations of Cu in the root system (76 ppm) compared to the live shoots (18 ppm) indicates the same barrier as for plants growing on tailings (Table 5). In contrast to the plants from the tailings, concentrations of Ni in dead shoots (4.9 ppm) are low compared to the root systems (13 ppm) and live shoots (9.0 ppm). Absorption of Ni in shoots continues after death on the tailings while in a natural habitat, Ni is released from the dead plant tissues.

4. Discussion

4.1. Metal release by sulfide oxidation

Dissolved metals in ground water are the central figures in the model of element cycling in the system "tailings–groundwater–plants" (Fig. 8). The concentration of dissolved metals is controlled by several processes such as the dissolution of primary sulfides, precipitation and dissolution of secondary minerals, the recrystallization of metastable phases, and the consumption of metals by plants (Fig. 8). The migration of the metals begins with the release of these cations from primary sulfides to the ground water as a result of oxidation. The initial hosts of Ni are Ni-bearing pyrrhotite and pentlandite, chalcopyrite for Cu, and sphalerite for Zn. The main source of Ni in the tailings is pyrrhotite because pentlandite is rare possibly due to a selective separation of sulfides during the flotation process. In the reduced zone, pyrrhotite has a rim of marcasite, showing the beginning of alteration (Fig. 4(a)). In the transition zone, pyrrhotite is surrounded by a vacant zone. Jambor (1994, 2003) found that the dark vacant zone usually contains traces of Fe-sulfate and native S in the atoll-type textures of

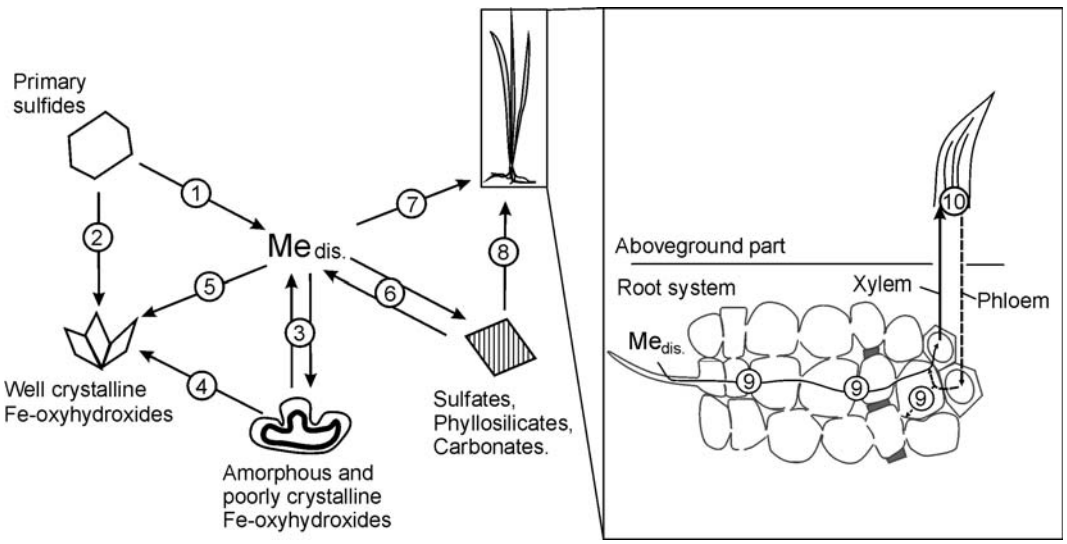

Fig. 8. A simplified model of metal behaviour in the system "mine tailings–ground water–plants". The processes are (1) dissolution of sulfides, (2) trapping of the metals during replacement of sulfides, (3) absorption/desorption from poorly crystalline phases, (4) absorption of crystalline phases during recrystallization of schwertmannite, (5) co-precipitation with goethite, lepidocrocite and jarosite, (6) precipitation/dissolution with soluble sulfates and adsorption/desorption on phyllosilicates and carbonates, (7) uptake of dissolved ions; (8) uptake by dissolution and ion exchange, (9) transport and absorption on the root cells and (10) absorption in cells of the shoot system.

pyrrhotite oxidation (Fig. 4(c)). These phases may have dissolved during the preparation of the polished sections and then the vacancy was filled with epoxy resin. Iron sulfates can be readily dissolved, causing Ni to migrate from pyrrhotite grains. However, further replacement of sulfide grains by Fe-hydroxides, such as goethite can allow the trapping of some metals in the solid phase (Fig. 8). More than 20% of the initial Ni from pyrrhotite remains in the rim as crystalline Fe-oxyhydroxides, such as goethite and lepidocrocite (Fig. 5(a) and (b)).

The supply of Ni, Cu and Zn to the groundwater will be dependant on the proportions of the initial hosts of the metals and the oxidation rate of specific sulfides, if the sulfides are assumed to have similar grain sizes. The proportions of sulfides can be estimated from the concentration of Ni, Cu, and Zn in the residual fraction after sequential extraction, as this represents the primary minerals. The mean concentration of metals in this fraction increases in the order Ni > Cu > Zn (Fig. 7 and Appendices 3–5), suggesting that the proportions of the sulfides are in the order Ni-pyrrhotite + pentlandite > chalcopyrite > sphalerite. The oxidation rates at pH 4 for pyrrhotite has been calculated to be $2.5–8.5 \times 10^{-9}$ mol m^{-2} s^{-1}, for sphalerite $4–6 \times 10^{-10}$ mol m^{-2} s^{-1}, and for chalcopyrite $8–17 \times 10^{-11}$ mol m^{-2} s^{-1} (Belize et al., 2004; Domènech et al., 2002). The high concentration of Ni-pyrrhotite and the rapid oxidation of this mineral compared to other sulfides produces the observed higher concentration of Ni than Zn and Cu in the groundwater. As the oxidation rate of chalcopyrite is slightly lower than for sphalerite, but the content of chalcopyrite was calculated to be higher from sequential extraction data (Appendices 4 and 5), the supply of Cu and Zn to the groundwater should be similar. However, Cu concentration is lower than Zn by several orders of magnitude (Table 3) indicating that other processes such as the precipitation of secondary minerals may exert a control on the concentration of these metals in the ground water.

4.2. Metal attenuation by Fe-oxyhydroxides and hydroxysulfates

Oxidation of Fe^{2+} to Fe^{3+} may actively occur in the pore water of the transition and oxidized zones above the water table. In the reduced zone, below the water table, oxidation would be slow due to the low coefficient of O_2 diffusion in tailings saturated with water (Elberling et al., 1994; Elberling and Damgaard, 2001). Hydrolysis of Fe^{3+} produces the precipitation of secondary Fe-oxyhydroxides, which can absorb other metals. Secondary Fe phases precipitate around calcite grains (Fig. 4(d)), because the dissolution of carbonate creates a local alkaline environment, which is favourable for the hydrolysis of Fe^{3+}.

The precipitation of jarosite, goethite, and ferrihydrite from ground water would be expected from the positive values of saturation indices. However, jarosite would not be expected at the observed pH of the groundwater (4.92–5.36) because it is only stable at pH < 3 (Bigham, 1994; Bigham and Nordstrom, 2000). The saturation index of schwertmannite is difficult to calculate numerically because logarithmic constants of apparent schwertmannite solubility vary by a factor of three between different studies (Kawano and Tomita, 2001; Bigham et al., 1996; Yu et al., 1999). However, calculated activities of SO_4^{2-} and Fe^{3+}, and the pH of the groundwater fall in the field of natural schwertmannite occurrence, while ferrihydrite would be expected to precipitate at a lower pH and activity of SO_4^{2-} than observed (Yu et al., 1999). From this deduction it can be concluded that only schwertmannite and goethite should precipitate from the groundwater. These phases were identified in precipitates forming from shallow groundwater exposed to air (Sidenko and Sherriff, 2005). Accumulation of S in the poorly crystalline Fe-phase at the bottom of the transition zone agrees with the mineralogical identification of schwertmannite $(Fe_8O_8(OH)_{8-2x}(SO_4)_x \cdot nH_2O)$. Here, at the fluctuating water table, precipitation of schwertmannite and goethite occurs due to oxidation of Fe^{2+} to Fe^{3+} by O_2 diffusing from the surface through unsaturated tailings.

Data from sequential extraction show a significant proportion of metals bound to the poorly crystalline Fe-phase, indicating the importance of schwertmannite in the attenuation of metals. Previous study showed that, most of the total Ni (99%) and Zn (53–94%) and a significant portion of Cu (33–76%) are bound to schwertmannite in precipitates forming from groundwater (Sidenko and Sherriff, 2005). Schwertmannite accumulates Ni, Cu and Zn in the transition zone (Fig. 7 and Appendices 3–5).

Schwertmannite is a metastable mineral which will re-crystallize completely into more stable goethite in about a year (Bigham et al., 1996). During this recrystallization, absorbed metals can be

released back into the solution or bound to the newly forming goethite (Fig. 8). This could be the cause of the gradual decrease of Ni, Cu and Zn in poorly-crystalline and their increase in well-crystalline Fe-oxyhydroxides from the bottom of the transition zone upward (Fig. 7). However, well-crystalline Fe phases might directly precipitate from solution without the intermediate formation of schwertmannite. The role of schwertmannite in the redistribution of metals, compared to crystalline goethite, becomes less important in the oxidized than in the transition zone.

Jarosite is another well-crystalline secondary mineral of Fe identified in the tailings. Jarosite might precipitate from pore water in the oxidized zone, which is usually more acidic (pH < 3) than the groundwater (Blowes and Ptaček, 1994). A comparison of Fe/S ratios in the well crystalline Fe phases indicates that only a few % of the total Fe could be bound to jarosite, and the major well crystalline phase is goethite.

The affinity of metals to well-crystallized secondary Fe-phases is shown by the mean proportions of the moderately reducible fraction from sequential extraction (Appendices 3–5), which decrease in the order Cu (18–34%) > Zn (17–21%) > Ni (8–13%). This order is the same as the affinity of the metals to goethite (Webster et al., 1998; Trivedi et al., 2001) and the sequence of element incorporation by jarosite (Dutrizac and Jambor, 2000). At the pH of the ground water (~5) adsorption edge studies have shown that Cu tends to be adsorbed onto secondary Fe phases while Zn and Ni stay in solution (Webster et al., 1998; Trivedi et al., 2001). This could be the reason for the concentrations of Zn being several orders of magnitude greater than Cu in the groundwater despite a similar flux of the metals from the dissolution of sphalerite and chalcopyrite in the tailings. Thus, the ability of Fe-oxyhydroxides and hydroxysulfates to remove specific metals is more likely to control their concentration in the ground water than the dissolution of host sulfides.

4.3. Available form of metals

The mean proportions of water-soluble metals from sequential extraction of the tailings are in the sequence Ni > Zn > Cu, which is opposite to that in stable crystalline Fe-oxyhydroxides (Appendices 3–5). It seems logical that if a metal can not be trapped in a stable form, it could possibly precipitate in a transient, more labile, form. As the concentration of water-soluble Cu is below detection limit, the formation of soluble Cu minerals would not be expected, while the significant concentrations of Ni and Zn in this fraction indicate that these metals could be incorporated into soluble minerals such as divalent metal sulfates. Soluble Ni and Zn sulfates are unlikely to precipitate from the ground water, as it is undersaturated with respect to them. However, Ni and Zn can co-precipitate with Fe and Mg sulfates due to structural similarities (Jambor et al., 2000; Gieré et al., 2003). The saturation indexes of melanterite ($FeSO_4 \cdot 7H_2O$) and epsomite ($MgSO_4 \cdot 7H_2O$) are slightly negative but close to zero. Therefore, these sulfates can precipitate if the groundwater evaporates becoming more saline. In most sections, the highest concentrations of soluble Fe, Ni and Zn were found in the transition zone, where the solution may become saturated with respect to Fe sulfates. Although sulfate minerals were not identified from this zone, the presence Ni-bearing melanterite in evaporites on the surface of the tailings supports the precipitation of Fe sulfates incorporating Zn and Ni.

Metals incorporated into water-soluble sulfates are more available for plants than those bound to exchangeable or carbonate fractions. The concentration of Ni and Zn in the water-soluble fraction is greater than in the exchangeable and carbonate fractions, while Cu does not accumulate in the soluble fraction (Appendices 3–5). Nevertheless, Cu in the exchangeable and carbonate fractions can be mobilized by the aminoacids of root exudates and then consumed by the plants (Salisbury and Ross, 1992). Exchangeable Cu could be incorporated into vermiculite (Dold and Fontboté, 2001), which was identified in weathered mica at the surface of tailings. Secondary Cu carbonates were not identified but Cu could be adsorbed on the surface of calcite (Compton and Pritchard, 1990).

4.4. Metal absorption by plants

The main inflow for metals into plants is from the soil via the root system (Brooks, 1983; Fergusson, 1990). Cations in the water-soluble fraction are the most readily available for roots, but cation exchange with solid phases becomes important if the metal concentration is low (Salisbury and Ross, 1992). Therefore, metals bound in exchangeable

and carbonate fractions of the solids can be considered as available forms (Kabata-Pendias and Pendias, 2001). The concentration of available metals in the tailings was calculated to be the sum of the water-soluble, exchangeable and carbonate fractions using the mean values from TR13. This region is similar to the plant collection area. The values of Zn (2.5 ppm) and Cu (1.8 ppm) available for plants from TR13 are similar to those in the natural soils (4.1 and 2.7 ppm, respectively). In contrast, the concentration of available Ni in natural soils is 14 ppm, which is 19 times less than for the tailings (270 ppm). The relative availability (available/total) of each metal was calculated as a ratio of the concentration in the available fraction to the total (Table 6). The relative availability of Ni is an order of magnitude greater than Cu and Zn for both the tailings (0.21) and the control areas (0.11). In the natural habitat, the relative availability of Cu (0.066) and Zn (0.056) is double that in the tailings (0.02 and 0.03), respectively, while for Ni it is half.

The relative absorption, which is the ratio between the metal concentration in the root system and in the available fraction (roots/available), indicates the nature of metal uptake by the root system. Within the tailings area, the relative order of metal uptake by the roots is Cu > Zn > Ni (Table 6). The concentration of Ni in the root systems was lower than in the available fraction of the tailings and natural soils, while the concentration of Cu and Zn in the roots was greater than the available metals (Table 6). Therefore, Cu and Zn penetrate into root cells against the concentration gradient, indicating active accumulation by plants (using energy). As the Ni concentration is lower in the roots, it most likely penetrates passively along the concentration gradient.

Table 6
Ratios of metal concentrations between the media and plant parts

	Ni	Cu	Zn
Delta tailings			
Available/total	0.21	0.020	0.030
Roots/available	0.86	18	8.5
Roots/total	0.18	0.36	0.26
Live shoots/roots	0.69	0.21	0.76
Dead shoots/live shoots	4.2	11	1.4
Dead shoots/total	0.53	0.84	0.28
Control area			
Available/total	0.11	0.066	0.056
Roots/available	0.93	28	7.6
Roots/total	0.11	1.8	0.45
Live shoots/roots	0.67	0.24	0.51
Dead shoots/live shoots	0.54	1.0	0.69
Dead shoots/total	0.038	0.46	0.16

Copper and Zn are micronutrients for plants (Chapin and Eviner, 2003; Marschner, 1995), which require 6 ppm Cu and 20 ppm Zn in their shoots for adequate plant growth (Epstein, 1965). Copper bound with enzymes participates in redox reactions, which relate to metabolic changes and plant growth. Copper enhances the permeability and lignification of cell walls and the viability of pollen. Copper deficiency causes stunted growth with distorted and bleached young leaves, and necrosis of apical meristems (regions of primary plant growth). Zinc has catalytic, cocatalytic, and structural functions in enzymes (Marschner, 1995). Zinc metalloproteins are involved in DNA replication and translation, hence affect gene expression. As a structural component of ribosomes, Zn is actively involved in protein synthesis. Zinc protects membrane lipids and proteins against oxidative damage by binding with phospholipid and sulfhydryl groups of membrane constituents, or by forming complexes with cysteine residues of polypeptide chains. There is an increase in plasma membrane permeability if Zn is deficient. The most visible symptoms of Zn deficiency are stunted growth and chlorosis. The high requirement of Cu and Zn for plant metabolism leads to their active uptake from the habitat.

The only biochemical function defined for Ni in plants is in the enzyme urease, which is an intermediate in N metabolism (Dixon et al., 1975; Marschner, 1995; Chapin and Eviner, 2003). Nickel is classified as a "beneficial nutrient", which can enhance plant growth, is required under specific conditions, or is necessary for specific plant groups (Dalton et al., 1985; Marschner, 1995; Chapin and Eviner, 2003). There is no clear evidence of Ni deficiency in plants (Dalton et al., 1985), although the critical concentration of Ni for barley shoots has been estimated to be around 0.1 ppm (Brown et al., 1990). There is much more concern about Ni toxicity levels, which begin at 10 ppm for sensitive crop species (Bollard, 1983; Asher, 1991). The minimal requirement of Ni by plants explains its passive uptake by water sedge growing in both tailings and control areas.

Inside the plant, cell membranes control the rates of ion absorption and the kinds of solutes

absorbed (Salisbury and Ross, 1992; Raven et al., 1999). Root cell membranes can decrease the flow of metals into the shoot system. Metals are transported from the root system by xylem flow to the cells of the shoot system, where they can be consumed by cells depending on the physiological needs of the plant or excreted from the shoots (Fig. 8). Some of the metals are returned to the roots by the flow of phloem. In the tailings area, the ratio of the concentration in the live shoots to the roots for Ni (0.69) and Zn (0.76) are about 3.5 times greater than for Cu (0.21). This difference in ratios shows that Ni and Zn move from roots to shoots more easily than Cu. In the control area, the concentration of metals in the shoots is much lower, but the character of Ni, Cu and Zn transfer from roots to shoots is the same as in the tailings (Table 5). Thus, Cu is absorbed by roots more effectively than Ni and Zn in both environments.

Copper is a transition element, which forms stable complexes and has a high affinity for peptide and sulfhydryl groups, carboxylic and phenol groups (Marschner, 1995). In plants receiving a large supply of Cu, transport of Cu from roots to the shoots is restricted. The concentration of Cu in the roots rises proportionately to that of the habitat, with up to 60% of the total Cu content being bound to the cell walls (Iwasaki et al., 1990). In contrast, root-supplied Zn is preferentially translocated to the shoot system to meet the high Zn requirements for normal growth of the plant (Kitagishi and Obata, 1986).

After the death of the shoots, metals can still penetrate into these organs via the root system because the dead shoots are still attached to the live roots. The concentration of Ni and Cu in the dead shoots of the sedge plants from the tailings was found to be even greater than in the root system (Table 5). This could be due to the absorption of metal ions by active groups of the organic compounds in the dead shoots. The ratio of the concentrations of metals in the dead to live shoots decreases in the order Cu (11) > Ni (4.2) > Zn (1.4), which reflects the adsorption affinity of the metals onto cellulose, the main component of the cell walls (Shukla and Pai, 2005). In the control area, the concentration of Ni in the dead shoot system is about half that of the live organs, but the concentration of Cu and Zn is equal (Table 5), indicating that Ni is released from dead shoots.

Shoot litter and root turnover form soil organic matter (Schlesinger, 1991). Nickel-rich dead shoots and roots in the tailings area would form contaminated litter. In boreal climates, only a small part of the organic C is decomposed during litter turnover, hence little Ni will be released back to the habitat with the rest being sequestered in the soil.

5. Conclusions

As a result of sulfide oxidation occurring in the Ni–Cu mine tailings at Thompson, metals are released from primary sulfides to the groundwater, where the pH is buffered at 5 by carbonate dissolution. Concentrations of Ni in the ground water are significantly greater than Cu and Zn because of (1) a high initial concentration of Ni in tailings; (2) a higher oxidation rate of Ni-bearing pyrrhotite compared to sphalerite and chalcopyrite; (3) the low affinity of Ni for secondary Fe phases. The co-precipitation of metals with Fe-oxyhydroxides and hydroxysulfates controls their attenuation from groundwater into a form unavailable for plants. The order of relative metal affinity for secondary Fe phases (Cu > Zn >Ni) is opposite to the order of availability of the elements (Ni > Zn > Cu).

Nickel penetrates passively from the tailings into the root system of water sedge, in contrast to Cu and Zn, which are actively absorbed micronutrients. Inside the plant, Ni and Zn can pass the barrier between the roots and shoots easier than Cu. After death, shoots of the plants from the tailings area continue to absorb metals in the order of their affinity to cellulose (Cu > Ni > Zn).

Acknowledgements

We thank the staff of the Environmental Health and Safety Office of INCO Ltd. Thompson Operations for field assistance, Ronald Chapman and Sergio Mejia for help with the SEM and EMP analysis. Thompson research was funded by a Collaborative Research and Development grant from NSERC, Canada, matched by INCO Ltd. Thompson Operations. Nikolay Sidenko was supported by a NATO–NSERC postdoctoral fellowship. We also thank Dr. Turnock, Dr. Wang, Dr. Cobb and Jared Etcheverry for helpful comments on this manuscript.

Appendix 1

Results of sequential extraction of Fe from solid samples of the tailings

Sample	Thickness (cm)	Zone	Total wt.%	Water-soluble		Exch. + carbon.		Am. Fe-hydrox.		Cry. Fe-hydrox.		Residual	
				wt.%	% of tot.	wt.%	% of tot.	wt.%	% of tot.	wt.%	% of tot.	wt.%	% of tot.
Section 1													
1/6	0–15	Ox	11	$<10^{-6}$	0	0.07	0.6	3.2	29	4.3	38	4	32
1/5	15–55	Ox	12	0.02	0.2	0.09	0.8	2.8	24	4.1	35	5	39
1/4	55–65	T1	14	0.07	0.5	0.23	1.6	3.1	22	1.1	8	10	68
1/3	65–80	T2	20	0.09	0.5	0.22	1.1	2.5	13	1.9	9	16	77
1/2	80–130	Rd	24	0.17	0.7	0.22	0.9	2.4	10	2.2	9	19	79
1/1	160–175	Rd	21	$<10^{-6}$	0	0.29	1.3	1.9	9	1.9	9	17	81
Weighted mean[a]			18	0.09	0.4	0.17	1.0	2.6	17	2.8	19	12	63
Section 4													
4/6	0–40	Ox	16	0.08	0.5	0.09	0.6	1.3	9	4.9	32	9	58
4/5	40–50	T1	13	0.05	0	0.17	1.3	1.7	13	1.8	14	9	71
4/4	50–70	T3	10	0.07	0.7	0.14	1.5	1.5	15	2.3	24	6	58
4/3	70–80	T4	18	0.14	0.8	0.28	1.6	3.8	21	2.0	11	12	65
4/2	80–100	Rd	19	$7 \cdot 10^{-5}$	0	0.26	1.4	2.3	12	1.8	9	14	77
4/1	160–175	Rd	13	$2 \cdot 10^{-5}$	0	0.17	1.3	1.8	14	0.9	7	10	78
Weighted mean[a]			15	0.06	0.4	0.16	1.1	1.8	13	2.9	20	10	66
Section 10													
10/5	0–25	Ox	16	0.10	0.6	0.16	1.0	3.1	19	5.2	31	8	48
10/4	25–45	T1	13	0.04	0.3	0.13	1.0	1.9	14	2.1	17	9	68
10/3	45–60	T2	14	0.13	0.9	0.17	1.2	1.9	13	2.4	17	10	67
10/2	60–70	T4	15	0.14	0.9	0.33	2.2	2.5	17	1.5	10	11	70
10/1	160–175	Rd	19	0.0004	0	0.25	1.3	2.8	15	1.2	7	15	77
Weighted mean[a]			15	0.08	0.5	0.19	1	2.5	16	2.8	19	10	64
Section 13													
13/5	0–7	Ox	16	0.03	0.2	0.08	0.5	2.1	14	5.5	35	8	51
13/4[b]	7–40	T2	9	0.13	1.4	0.02	0.2	1.5	16	2.1	23	6	61
13/3	40–45	T4	13	0.00	0.03	0.08	0.6	2.2	17	1.1	9	9	74
13/2	45–60	Rd	12	0.04	0.3	0.11	0.9	1.8	14	1.2	10	9	74
13/1	160–175	Rd	13	0.07	0.6	0.10	0.8	2.1	17	1.3	11	9	71
Weighted mean[a]			12	0.08	0.8	0.07	0.5	1.8	16	2.0	18	8	66

[a] The mean element content of each cross-section was weighted by the thickness of the sample interval.

[b] The mean of triplicate analyses (see Table 1).

Appendix 2

Results of sequential extraction of S from solid samples of the tailings

Sample	Thickness (cm)	Zone	Total ppm	Water-soluble		Exch. + carbon.		Am. Fe-hydrox.		Cry. Fe-hydrox.		Residual	
				wt.%	% of tot.	wt.%	% of tot.	wt.%	% of tot.	wt.%	% of tot.	wt.%	% of tot.
Section 1													
1/6	0–15	Ox	2.6	0.3	11	0.03	1.1	0.03	1.0	0.12	4.5	2	83
1/5	15–55	Ox	3.6	0.4	12	0.05	1.4	0.05	1.4	0.10	2.8	3	82
1/4	55–65	T1	6.7	0.5	7	0.07	1.0	0.09	1.4	0.02	0.3	6	90
1/3	65—80	T2	10.2	0.6	6	0.07	0.7	0.07	0.7	0.04	0.4	9	92
1/2	80–130	Rd	10.4	0.7	7	0.10	1.0	0.06	0.6	0.04	0.4	9	91
1/1	160–175	Rd	11.3	0.4	4	0.04	0.3	0.04	0.4	0.04	0.3	11	95
Weighted mean[a]			7.5	0.5	8	0	1.0	0.06	0.9	0.06	1.5	7	88
Section 4													
4/6	0–40	Ox	5.2	0.3	7	0.03	0.6	0.03	0.6	0.13	2.5	5	90
4/5	40–50	T1	5.9	0.5	8	0.04	0.6	0.04	0.7	0.06	1.1	5	90
4/4	50–70	T3	3.8	0.6	15	0.07	1.9	0.07	1.9	0.09	2.2	3	79
4/3	70–80	T4	8.5	0.9	11	0.12	1.4	0.23	2.7	0.07	0.8	7	84
4/2	80–100	Rd	9.7	0.7	7	0.04	0.5	0.06	0.7	0.03	0.3	9	91
4/1	160–175	Rd	6.7	0.5	7	0.03	0.4	0.03	0.4	0.03	0.5	6	91
Weighted mean[a]			6.3	0.5	9	0.05	0.9	0.06	1.0	0.08	2	6	88
Section 10													
10/5	0–25	Ox	5.5	0.5	8	0.05	1.0	0.04	0.8	0.12	2.2	5	88
10/4	25–45	T1	5.9	0.4	8	0.03	0.6	0.03	0.5	0.07	1.2	5	90
10/3	45–60	T2	6.8	0.5	7	0.06	0.9	0.07	1.1	0.09	1.3	6	90
10/2	60–70	T4	7.9	0.7	9	0.11	1.4	0.18	2.2	0.05	0.6	7	87
10/1	160–175	Rd	10.9	0.5	4	0.03	0.3	0.06	0.5	0.03	0.3	10	95
Weighted mean[a]			7.1	0.5	7	0.05	1	0.06	0.9	0.08	1	6	90
Section 13													
13/5	0–7	Ox	5.4	0.9	16	0.03	0.6	0.06	1.1	0.10	1.9	4	80
13/4[b]	7–40	T2	5.0	0.5	10	0.02	0	0.03	0.5	0.07	1	4	88
13/3	40–45	T4	5.8	0.8	14	0.06	0.9	0.08	1.3	0.07	1.2	5	83
13/2	45–60	Rd	5.9	0.6	10	0.04	0.7	0.06	1.0	0.04	0.6	5	88
13/1	160–175	Rd	6.2	0.7	11	0.06	0.9	0.05	0.8	0.03	0.5	5	87
Weighted mean[a]			5.5	0.6	11	0.04	1	0.04	0.8	0.06	1	5	87

[a,b] See note for Appendix 1.

Appendix 3

Results of sequential extraction of Ni from solid samples of the tailings

Sample	Thickness (cm)	Zone	Total ppm	Water-soluble		Exch. + carbon.		Am. Fe-hydrox.		Cry. Fe-hydrox.		Residual	
				ppm	% of tot.	ppm	% of tot.	ppm	% of tot.	ppm	% of tot.	ppm	% of tot.
Section 1													
1/6	0–15	Ox	900	29	3	57	6	220	24	230	26	360	40
1/5	15–55	Ox	1200	130	11	60	5	160	13	270	23	570	48
1/4	55–65	T1	2500	540	22	140	6	370	15	150	6	1300	52
1/3	65–80	T2	3500	680	19	118	3	280	8	210	6	2210	63
1/2	80–130	Rd	3700	490	13	136	4	220	6	210	6	2640	71
1/1	160–175	Rd	3200	30	1	150	5	300	9	260	8	2460	77
Weighted mean[a]			2500	310	11	107	5	228	11	230	13	1678	60
Section 4													
4/6	0–40	Ox	2170	330	15	72	3	130	6	210	10	1430	66
4/5	40–50	T1	2620	240	9	66	3	140	5	160	6	2010	77
4/4	50–70	T3	1550	330	21	78	5	90	6	150	10	900	58
4/3	70–80	T4	3370	740	22	221	7	460	14	170	5	1780	53
4/2	80–100	Rd	2970	90	3	135	5	260	9	190	6	2300	77
4/1	160–175	Rd	1980	130	7	107	5	300	15	90	5	1350	68
Weighted mean[a]			2300	290	13	101	4	197	8	173	8	1560	67
Section 10													
10/5	0–25	Ox	2800	250	9	91	3	180	6	310	11	1970	70
10/4	25–45	T1	2600	200	8	70	3	170	7	200	8	1960	75
10/3	45–60	T2	3000	400	13	74	2	200	7	200	7	2130	71
10/2	60–70	T4	3300	420	13	152	5	450	14	180	5	2100	64
10/1	160–175	Rd	2800	4.4	0	115	4	350	13	100	4	2230	80
Weighted mean[a]			2900	240	8	95	3	243	8	212	8	2057	73
Section 13													
13/5	0–7	Ox	1800	380	21	58	3	190	11	230	13	940	52
13/4[b]	7–40	T2	1200	250	20	20	2	80	7	130	10	720	62
13/3	40–45	T4	1900	430	23	121	6	350	18	46	2	950	50
13/2	45–60	Rd	1600	250	16	66	4	190	12	77	5	1020	64
13/1	160–175	Rd	2300	330	14	73	3	200	9	120	5	1580	69
Weighted mean[a]			1600	290	18	50	3	154	9	121	8	988	62

[a,b] See note for Appendix 1.

Appendix 4

Results of sequential extraction of Cu from solid samples of the tailings

Sample	Thickness (cm)	Zone	Total ppm	Water-soluble		Exch. + carbon.		Am. Fe-hydrox.		Cry. Fe-hydrox.		Residual	
				ppm	% of tot.	ppm	% of tot.	ppm	% of tot.	ppm	% of tot.	ppm	% of tot.
Section 1													
1/6	0–15	Ox	140	<0.1	0	7.8	5.5	19	14	110	79	3	2
1/5	15–55	Ox	150	<0.1	0	5.5	3.7	14	9	100	67	31	21
1/4	55–65	T1	190	<0.1	0	3.0	1.6	10	5	16	8	160	84
1/3	65–80	T2	200	<0.1	0	1.8	0.9	35	18	15	8	150	75
1/2	80–130	Rd	230	<0.1	0	6.2	2.7	21	9	33	14	170	74
1/1	160–175	Rd	170	<0.1	0	1.2	0.7	30	18	15	9	120	71
Weighted mean[a]			190	<0.1	0	5.0	2.8	21	11	55	34	106	52
Section 4					0								
4/6	0–40	Ox	230	<0.1	0	4.8	2.1	9	4	65	28	150	65
4/5	40–50	T1	170	<0.1	0	4.0	2.3	29	17	28	17	110	65
4/4	50–70	T3	210	<0.1	0	8.8	4.2	20	9	38	18	140	67
4/3	70–80	T4	210	<0.1	0	4.5	2.1	37	18	22	11	150	71
4/2	80–100	Rd	180	<0.1	0	1.5	0.8	27	15	24	14	130	72
4/1	160–175	Rd	200	<0.1	0	2.8	1.4	30	15	9	4	160	80
Weighted mean[a]			210	<0.1	0	4.6	2.2	21	11	39	18	143	69
Section 10					0								
10/5	0–25	Ox	230	<0.1	0	4.3	1.9	12	5	94	41	120	52
10/4	25–45	T1	200	<0.1	0	4.7	2.3	22	11	58	29	120	60
10/3	45–60	T2	230	<0.1	0	4.1	1.8	23	10	42	18	160	70
10/2	60–70	T4	200	<0.1	0	2.5	1.3	41	21	23	11	130	65
10/1	160–175	Rd	210	<0.1	0	0.8	0.4	28	13	10	5	170	81
Weighted mean[a]			220	<0.1	0	3.5	1.6	23	11	53	24	137	64
Section 13													
13/5	0–7	Ox	110	<0.1	0	1.8	1.6	13	11	63	57	33	30
13/4[b]	7–40	T2	130	<0.1	0	1.8	1.6	3.1	2.8	35	31	90	65
13/3	40–45	T4	110	<0.1	0	4.4	4.0	19	17	1	1	86	78
13/2	45–60	Rd	120	<0.1	0	2.2	1.8	14	11	13	11	91	76
13/1	160–175	Rd	110	<0.1	0	2.5	2.2	14	13	13	12	80	73
Weighted mean[a]			120	<0.1	0	2.2	1.9	9	8	27	24	83	66

[a,b] See note for Appendix 1.

Appendix 5

Results of sequential extraction of Zn from solid samples of the tailings

Sample	Thickness (cm)	Zone	Total ppm	Water-soluble		Exch. + carbon.		Am. Fe-hydrox.		Cry. Fe-hydrox.		Residual	
				ppm	% of tot.	ppm	% of tot.	ppm	% of tot.	ppm	% of tot.	ppm	% of tot.
Section 1													
1/6	0–15	Ox	71	<0.1	0	0.8	1.2	11	15	22	31	37	53
1/5	15–55	Ox	72	<0.1	0	0.6	0.9	11	15	24	33	37	51
1/4	55–65	T1	82	3.3	4.0	2.2	2.7	24	29	9	11	43	53
1/3	65–80	T2	100	4.1	4.1	1.8	1.8	10	10	12	12	72	72
1/2	80–130	Rd	92	2.8	3.0	1.4	1.5	8	8	11	12	69	75
1/1	160–175	Rd	93	<0.1	0	2.4	2.6	11	12	14	15	66	70
Weighted mean[a]			85	1.6	1.7	1.3	1.5	11	13	16	20	55	64
Section 4													
4/6	0–40	Ox	79	1.8	2.3	0.7	0.9	6	8	19	25	51	64
4/5	40–50	T1	88	1.5	1.7	1.3	1.5	11	13	12	14	62	70
4/4	50–70	T3	74	3.0	4.0	1.6	2.2	11	14	14	19	44	60
4/3	70–80	T4	100	6.4	6.4	2.7	2.7	24	24	13	13	54	54
4/2	80–100	Rd	97	<0.1	0	2.0	2.1	10	11	11	12	73	76
4/1	160–175	Rd	76	<0.1	0	1.5	2.0	10	14	7	9	58	75
Weighted mean[a]			84	1.8	2.2	1.4	1.7	10	12	14	17	56	67
Section 10													
10/5	0–25	Ox	93	1.5	1.6	1.0	1.0	12	13	28	30	50	54
10/4	25–45	T1	90	1.2	1.3	1.1	1.3	12	13	17	19	59	66
10/3	45–60	T2	84	2.4	2.9	0.9	1.1	9	11	13	16	58	69
10/2	60–70	T4	88	3.6	4.0	2.0	2.3	16	19	10	11	57	64
10/1	160–175	Rd	105	<0.1	0	2.0	1.9	18	17	10	9	75	72
Weighted mean[a]			92	1.6	1.8	1.3	1.4	13	14	17	19	59	64
Section 13													
13/5	0–7	Ox	80	1.9	2.4	0.7	0.9	10	13	26	33	41	51
13/4[b]	7–40	T2	68	1.7	2.4	0.9	1.4	12	17	21	31	33	48
13/3	40–45	T4	100	1.9	1.9	1.3	1.3	17	17	6	6	74	74
13/2	45–60	Rd	100	1.4	1.4	1.4	1.4	16	16	11	11	70	71
13/1	160–175	Rd	83	1.6	2.0	0.9	1.1	10	12	8	10	62	75
Weighted mean[a]			81	1.6	2.1	1.0	1.3	12	15	16	21	50	60

[a,b] See note for Appendix 1.

References

Asher, C.J. 1991. Beneficial elements, functional nutrients, and possible new essential elements. In: Mortvedt, F.R., Shuman, L.M., Welch R.M. (Eds.), Micronutrients in Agriculture. Soil Sci. Soc, Am. Book Series No. 4, Madison, Wi, USA. pp. 703–723.

Ball, J.W., Nordstrom, D.K., 1991. User's manual for WATEQ4f, with revised thermodynamic data base and test cases for calculating speciation of major, trace, and redox elements in natural waters. US. Geol. Surv. Open-File Rep. pp. 91–183.

Belize, N., Chen, Y.-W., Cai, M.-F., Li, Y., 2004. A review on pyrrhotite oxidation. J. Geochem. Explor. 84, 65–76.

Bigham, J.M., 1994. Mineralogy of ochre deposits formed by sulphide oxidation. In: Jambor, J.L., Blowes, D.W. (Eds.), Short Course Handbook on Environmental Geochemistry of Sulphide Mine Waste. Mineral. Assoc. Can., Waterloo, pp. 103–132.

Bigham, J.M., Nordstrom, D.K., 2000. Iron and aluminium hydroxysulfates from acid sulfate waters. In: Alpers, N.C., Jambor, J.L., Nordstrom, D.K. (Eds.), Sulfate Minerals: Crystallography, Mineralogy And Environmental Significance, 40. Rev. Mineral. Geochem., pp. 351–404.

Bigham, J.M., Schwertmann, U., Tarina, S.J., Winland, R.L., Wolf, M., 1996. Schwertmannite and the chemical modeling of iron in acid mine waters. Geochim. Cosmochim. Acta 60, 2111–2121.

Blowes, D.W., Ptaček, C.J., 1994. Acid-neutralization mechanisms in inactive mine tailings. In: Jambor, J.L., Blowes, D.W. (Eds.), Short course handbook on Environmental geochemistry of sulfide mine waste, 22. Mineral. Assoc. Can. Short Course Ser., pp. 271–292.

Bock, R., 1984. A handbook of decomposition methods in analytical chemistry. Khimiya, Moscow (in Russian).

Bollard, E.G., 1983. Involvement of unusual elements in plant growth and nutrition. In: Läuchli, A., Bieleski, R.L. (Eds.), Encyclopedia of Plant Physiology New Series, 15B. Springer-Verlag, Berlin and New York, pp. 695–755.

Bradbeer, J.W., 1988. Seed dormancy and germination. Chapman and Hall, New York.

Brooks, R.R., 1983. Biological Methods of Prospecting for Minerals. Wiley, New York.

Brown, P.H., Welch, R.M., Madison, J.T., 1990. Effect of nickel deficiency on soluble anion, amino acid, and nitrogen levels in barley. Plant Soil 125, 19–27.

Chao, T.T., Zhou, L., 1983. Extraction techniques for selective dissolution of amorphous iron oxides from soils and sediments. J. Soil Sci. Am. Proc. 47, 225–232.

Chapin III, F.S., Eviner, V.T., 2003. Biogeochemistry of terrestrial Net Primary Production. In: Schlesinger, W.H. (Ed.), Biogeochemistry. In: Holland, H.D., Turekian, K.K. (Eds.), Treatise on Goechemistry, 8. Elsevier Pergamon, Oxford, pp. 215–247.

Cobb, G.P., Sands, K., Waters, M., Wixson, B.G., Dorward-King, E., 2000. Accumulation of heavy metals by vegetables grown in mine wastes. Environ. Toxicol. Chem. 19, 600–607.

Compton, R.G., Pritchard, K.L., 1990. Kinetics of the Langmuirian adsorption of Cu(II) ions at the calcite water interface. J. Chem. Soc.–Faraday Trans. 86, 129–136.

Dalton, D.A., Evans, H.J., Hanus, F.J., 1985. Stimulation by nickel of soil microbial urease activity and urease and hydrogenase activity in soybeans grown in a low-nickel soil. Plant Soil 88, 245–258.

Dixon, N.E., Gazola, C., Blakeley, R.L., Zerner, B., 1975. Jack bean urease (EC 3.5.1.5.), a metalloenzyme. A simple biological role for nickel? J. Am. Chem. Soc. 97, 4131–4133.

Dold, B., 2003a. Speciation of the most soluble phases in a sequential extraction procedure adapted for geochemical studies of copper sulfide mine waste. J. Geochem. Explor. 80, 55–68.

Dold, B., 2003b. Dissolution kinetics of schwertmannite and ferrihydrite in oxidized mine samples and their detection by differential X-ray diffraction (DXRD). Appl. Geochem. 18, 1531–1540.

Dold, B., Fontboté, L., 2001. Element cycling and secondary mineralogy in porphyry copper mine tailings as a function of climate, primary mineralogy and mineral processing. J. Geochem. Explor. 74, 3–55.

Domènech, C., de Pablo, J., Ayora, C., 2002. Oxidative dissolution of pyritic sludge from the Aznalcóllar mine (SW Spain). Chem. Geol. 190, 339–353.

Dutrizac, J.E., Jambor, J.L., 2000. Jarosites and their application in hydrometallurgy. In: Alpers, C.N., Jambor, J.L., Nordstrom, D.K. (Eds.), Sulfate minerals: Crystallography Mineralogy and Environmental Significance, vol. 40. Rev. Mineral. Geochem., pp. 405–453.

Elberling, B., Damgaard, L.R., 2001. Microscale measurements of oxygen diffusion and consumption in subaqueous sulphide tailings. Geochim. Cosmochim. Acta 65, 1897–1905.

Elberling, B., Nicholson, R.V., Reardon, E.J., Tibble, P., 1994. Evaluation of sulphide oxidation rates: a laboratory study comparing oxygen fluxes and rates of oxidation product release. Can. Geotech. J. 31, 375–383.

Epstein, E., 1965. Mineral metabolism. In: Bonner, J., Varner, J.E. (Eds.), Plant Biochemistry. Academic Press, London, pp. 38–466.

Fanfani, L., Zuddas, P., Chessa, A., 1997. Heavy metals speciation analysis as a tool for studying mine tailings weathering. J. Geochem. Explor. 58, 241–248.

Fergusson, J.E., 1990. The heavy elements: chemistry, environmental impact and health effects. Pergamon Press, New York.

Gieré, R., Sidenko, N.V., Lazareva, E.V., 2003. The role of secondary minerals in controlling the migration of arsenic and metals from high-sulfide wastes (Berikul gold mine, Siberia). Appl. Geochem. 18, 1347–1359.

Hall, G.E.M., Vaive, J.E., Beer, R., Hoashi, M., 1996. Selective leaches revisited, with emphasis on the amorphous Fe oxyhydroxides phase extraction. J. Geochem. Explor. 56, 59–78.

Iwasaki, K., Sakurai, K., Takahashi, E., 1990. Copper binding by the root cell walls of Italian ryegrass and red clover. Soil Sci. Plant Nutr. (Tokyo) 36, 431–440.

Jambor, J.L., 1994. Mineralogy of sulfide rich tailings and their oxidation products. In: Jambor, J.L., Blowes, D.W. (Eds.), Short course handbook on Environmental geochemistry of sulfide mine waste, vol. 22. Mineral. Assoc. Can. Short Course Ser., pp. 59–102.

Jambor, J.L., 2003. Mine waste mineralogy and mineralogical perspectives of acid–base accounting. In: Jambor, J.L., Blowes, D.W., Ritchie, A.M.I. (Eds.), Environmental aspects of mine waste. Mineral, vol. 31. Assoc. Can. Short Course Ser., pp. 117–147.

Jambor, J.L., Nordstrom, D.K., Alpers, C.N., 2000. Metal sulfate salts from sulfide mineral oxidation. In: Alpers, C.N., Jambor, J.L., Nordstrom, D.K. (Eds.), Sulfate minerals: Crystallography, Mineralogy and Environmental Significance, vol. 40. Rev. Mineral. Geochem., pp. 305–340.

Johnson, R.H., Blowes, D.W., Robertson, W.D., Jambor, J.L., 2000. The hydrogeochemistry of Nickel Rim mine tailings impoundment, Sudbury, Ontario. J. Contam. Hydrol. 41, 49–80.

Kabata-Pendias, A., Pendias, H., 2001. Trace elements in soils and plants. CRC Press, Boca Raton, New York.

Kavalench, J., 2004. Mineralogy and Geochemistry of Hardpan in Ni–Cu tailings at INCO Ltd., Thompson Manitoba. B.S. thesis. University of Manitoba, Winnipeg.

Kawano, M., Tomita, K., 2001. Geochemical modeling of bacterially induced mineralization of schwertmannite and jarosite in sulfuric acid spring. Am. Mineral. 86, 1159–1165.

Khozhina, E.I., 2002. Migration of heavy metals in biogeosystem of technogenic lakes of Salair ore-refining plant, Kemerovo region. Ph.D. Thesis. United Institute of Geology, Geophysics, and Mineralogy, Novosibirsk, Russia (in Russian).

Kitagishi, K., Obata, H., 1986. Effects of zinc deficiency on the nitrogen metabolism of meristematic tissues of rice plants with reference to protein synthesis. Soil Sci. Plant Nutr. (Tokyo) 32, 397–405.

Koval, S.F., Shamanin, V.P., 1999. Rastenie v opyte (Plant in an experiment). OmGAU, Omsk (in Russian).

Klohn Leonoff, 1992. Thompson Tailings Management Plan prepared for INCO Ltd, Manitoba Division, by Klohn Leonoff Ltd, December 31, 1992 (unpublished report).

Lierop, W.V., 1990. Soil pH and lime requirement determination. In: Westerman, R.L. (Ed.), Soil testing and plant analysis, third ed. Soil Science Society of America, Inc., Madison, Wisconsin, USA, pp. 73–126.

Marques, M.J., Martinez-Conde, E., Rovira, J.V., Ordonez, S., 2001. Heavy metals pollution of aquatic ecosystems in the vicinity of a recent closed underground lead–zinc mine (Basque County, Spain). Environ. Geol. 40, 1125–1137.

Marschner, H., 1995. Mineral Nutrition of Higher Plants. Academic Press Ltd., Toronto.

McGregor, R.G., Blowes, D.W., Robertson, W.D., 1995. The application of chemical extractions to sulfide tailings at the Copper Cliff tailings area, Sudbury, Ontario. In: Hynes, T.P., Blanchette, M.C. (Eds.), Sudbury '95 – Mining and the Environment, Vol. 3. CANMET, Ottawa, Canada, pp. 133–1142.

Moore, D.M., Reynolds Jr., R.C., 1997. X-ray diffraction and the identification and analysis of clay minerals. Oxford University Press, New York.

Newman, D.R., Vandeberg, G.S., Blicker, P.B., Goering, J.D., Jennings, S.R., Ford, K., 2005. Phytostabilization of acid metalliferous mine tailings at the Keating Site in Montana. In: Proc. National Meeting of the American Society of Mining and Reclamation, 2005. ASMR. Lexington, KY. (June 19–23).

Raven, P.H., Evert, R.F., Eichhorn, S.E., 1999. Biology of Plants. Worth Publishers, New York.

Ribet, I., Ptacek, C.J., Blowes, D.W., Jambor, J.L., 1995. The potential for metal release by reductive dissolution of weathered mine tailings. J. Contam. Hydrol. 17, 239–273.

Salisbury, F.B., Ross, C.W., 1992. Plant Physiology. Wadsworth Publishing Company, Belmont, California.

Schlesinger, W.H., 1991. Biogeochemistry: an Analysis of Global Change. Academic Press, San Diego.

Shukla, S.R., Pai, R.S., 2005. Adsorption of Cu(II), Ni(II), and Zn(II) on dye loaded groundnut shells and sawdust. Separat. Puriffic. Thech. 43, 1–8.

Sidenko, N.V., Sherriff, B.L., 2005. The attenuation of Ni, Zn, Cu, by secondary Fe phases from surface and ground water of two sulfide mine tailings in Manitoba, Canada. Appl. Geochem. 20, 1180–1194.

Sidenko, N.V., Bortnikova, S.B., Lazareva, E.V., Kireev, A.D., Sherriff, B.L., 2005. Geochemical and mineralogical zoning of high-sulfide mine waste at the Berikul mine site, Kemerovo region, Russia. Can. Miner. 43, 1141–1156.

SRK, 1984. Rock Mechanics Study, Thompson Open Pit. Appendix A-Geology (unpublished report).

Tan, K.H., 1996. Soil Sampling, Preparation and Analysis. Marcel Dekker Inc., New York.

Tessier, A., Cambell, P.G.C., Bisson, M., 1979. Sequential extraction procedure for the the speciation of particulate trace metals. Anal. Chem. 51, 256–273.

Tisch, B., Beckett, P., Courtin, G., Payne, R., 1999. Reclamation Activities at the Pronto Copper Tailings near Elliot Lake. In: Mawhinney, A.-M., Pitblado, J. (Eds.), Boom Town Blues: Collapse and Revival in a Single-Industry Community. Dundurn Press, Toronto, pp. 305–318.

Trivedi, P., Axe, L., Dyer, J., 2001. Adsorption of metal ions onto goethite: single-adsorbate and competitive systems. Coll. Surfaces, Sect. A 191, 107–121.

Webster, J.G., Swedlund, P.J., Webster, K.S., 1998. Trace metal adsorption onto and acid mine drainage iron (III) oxyhydroxysulfate. Environ. Sci. Technol. 32, 1361–1368.

Winterhalder, K., 1995. Dynamics of plant communities and soils in revegetated ecosystems – a Sudbury case study. In: Gunn, J. (Ed.), Environmental Restoration and Recovery of an Industrial region. Springer-Verlag, New York, pp. 173–182.

Yu, J.-Y., Heo, B., Choi, I.-K., Cho, J.-P., Chang, H.-W., 1999. Apparent solubilities of schwertmannite and ferrihydrite in natural stream waters polluted by mine drainage, Geochim. Cosmochim. Acta B63, 3407–3416.